On predicting the deformation and fracture properties of ABS / PMMA / Nano-SiO2 composites

Jin Ding (happyflower1221@163.com)
Shandong University
Yahui Huang
Shandong University
Zhenshan Fu
Shandong University
Wenchao Cui
Shandong University

Research Article

Keywords: ABS/PMMA/nano-SiO2 composites, Damage mechanics, Representative Volume Elements(RVEs), Elastoplastic-damage

Posted Date: April 19th, 2021

DOI: https://doi.org/10.21203/rs.3.rs-411182/v1

On predicting the deformation and fracture properties of ABS / PMMA / Nano -SiO_2 composites

Jin Ding[1], Yahui Huang[2], Zhenshan Fu[1],Wenchao Cui[1*]

[1] *Naval Architecture and Port Engineering College, Shandong jiaotong University, 1508 Chuangxing Road, Weihai, 264209, China*

[2] *School of Mechanical, Electrical and Information Engineering, Shandong University, 180 Wenhuaxi Road,Weihai , 264209, China*

Abstract:

The damage mechanism of ABS/PMMA/nano-SiO_2 composites was studied by both experiments and finite element analysis in this paper. A microstructure-based the Homogenization theory and the surface-based cohesive method was developed to predict the deformation and fracture behavior of ABS/PMMA/nano-SiO_2 composite. The constitutive behavior of the elastoplastic-damage in the matrix, the fracture for the nano-SiO_2 reinforement , and the traction-separation for interfaces, were simulated in this model. The validity of the modeling results were validated by the agreement of the experiment and the morphology of fracture section with those predicted by the simulation. The numerical results were used to provide insight into the damage mechamisms of ABS/PMMA/nano-SiO_2 composites, and the effects of nano-SiO_2 strength on ABS/PMMA blends mechanical properties were also discussed in detail.

Keywords: ABS/PMMA/nano-SiO_2 composites. Damage mechanics.Representative Volume Elements(RVEs). Elastoplastic-damage

1 Introduction

Acrylonitrile-butadiene styrene (ABS), as a type of excellent rubber-toughened thermoplastic, has been widely used in many fields for many years such as automotive and household appliance industries due to its good processability, low water absorption, and high impact strength. However, neat ABS materials usually have low toughness and surface glossiness. Polymer blends have recently drawn considerable interest because these materials present outstanding properties at low cost. ABS/poly (methyl methacrylate) (PMMA) blends are characterized by a remarkable combination of physical properties, such as excellent surface glossiness, easy processability, and high mechanical strength. At the same time, the blends toughness is declined because of the inherent brittleness of PMMA [1-6]. It is difficult to toughen and stiffen polymeric matrix simultaneously through physical blending as well as know.

In recent years, using inorganic nanoparticles as modifiers to refine the morphology of polymer blends has received considerable attention. Compared with traditional microcomposites, the massive surface to volume ratio of the nanoparticles results in a big interfacial area and a high surface energy of nanoparticle fillers, which lead to a strong interfacial adhesion between polymeric matrix and the fillers and hence affects the properties of the overall composites[7]. There are generally two methods that have been used to study the mechanical behavior of the polymer modified with nanoparticles: experimental approach and numerical modeling. Many experimental studies describe the effects of nanoparticles in polymer blends [8-14].Mu et al. [15] investigated the effects of SiO_2 on the morphology of micro PMMA and found that

nano-SiO_2 particles could grow on PMMA microspheres. Haghtalab and Rahimi [16] studied the effects of ABS and nanosilica with different nanoparticle sizes and various loadings. Zhang et al.[8] investigated of nano-$CaCO_3$ on the rheological and mechanical properties of ABS/PMMA blends, the results showed that the tensile yield strength decreased slightly with the increase in nano-$CaCO_3$ content, and all nano-$CaCO_3$ particles significantly decrease the Izod impact strength. In our previous experimental study, we have investigated the influence of nano-SiO_2 particle modification on the morphology and properties of ABS/PMMA polymer blends.When the contents of the nano-SiO_2 fillers were below 2wt%, the toughness of the ternary blends was significantly improved [17]. These researches proved that nanoparticles and high filler loadings enhanced the nanoparticle surface area and the viscoelastic properties were intensified by increasing the polymer chain adsorption on the nanoparticles. However, the experimental approach can not characterize the actual interactions that occur between the polymer matrix, the modifier, and the interfaces during deformation and fracture processes.

In the numerical modeling of polymer nanoparticles composites, there exist two popular methods: discrete element method (DEM) and finite element method(FEM).The DEM model has a faster convergence rate than FEM, however ,it neglects some important factors that are necessary for the study of deformation and fracture mechanisms in polymer nanoparticles composites, such as the geometry of the particles, the brittle fracture between the matrix and the particles. FEM is often used to fully reconstruct the microstructure of the composite materials, including the

irregular morphology of the particles, the inhomogeneous spatial distribution of particles and the anisotropy of properties in the particles. In the literatures there have been a few effective numerical models based on FEM proposed to study the mechanical properties of polymer composites. For example, based on sensitivity analysis (SA) methods, N.vuBac et al. [18] proposed a stochastic framework to quantify the key-input parameters influencing the Yong's modulus of polymer (epoxy) clay nanocomposites (PCNs). All stochastic methods predict that the key parameters for Yong's modulus are the epoxy stiffness followed by the clay volume fraction. Pontefisso et al.[12] developed a new algorithm for the generation of 3D Representative Volume Elements(RVEs),which is easy to be meshed and imported in a FE code. The interphase thickness and properties on the elastic properties of nanocomposites was studied with a computational analysis .Yuan [13] studied the effects of nanofiller content on the interfacial properties in polymer blend nanocomposites based on the micromechanical modeling of experimental tensile strength and modulus. The calculated results showed that the good interfacial properties in the samples containing low nanofiller concentrations.

Although there are previous studies explicitly considering the fracture behavior of composite using FEM method, they are not able to account for the effect of nanoparticle morphology on the properties of ABS/PMMA/nano-SiO_2 polymer blends. Since these models are established based on spherical particle assumption, meanwhile, the multiphase failure of particles was not taken into account in these models. The remainder of the paper is organized as follows. In Section 2, the Homogenization

theory and the surface-based cohesive method are described briefly. Section 3 presents the materials and the experimental procedures. Section 4 presents a microstructure-based finite element model to predict the interfacial debonding of ABS/PMMA/nano-SiO_2 polymer blends. We validate the model by challenging it with experimental data in Section 5. Finally, some conclusion, and potential extension are discussed in Section 6.

2 Micromechanical design theory guidelines

2.1 Homogenization theory

The Homogenization theory is widely used in converting inhomogeneous composite into homogeneous material. It often relies on the finite element method to simulate the response of the samples discretely with four-node quadrangle elements and three-node triangular elements. Four edges of RVE are defined as periodic boundary conditions. To minimize the effect of the mesh density, it was kept very fine.

The equivalent elastic constant tensor of composite (C_{ijkl}) as follows：

$$\bar{\sigma}_{ij} = C_{ijkl}\bar{\varepsilon}_{ij} \tag{1}$$

where $\bar{\sigma}_{ij}$ is the mean stress, and $\bar{\varepsilon}_{ij}$ is the mean strain of a unit cell $\bar{\varepsilon}_{ij}$, $\bar{\sigma}_{ij}$ and $\bar{\varepsilon}_{ij}$ are calculated as follows：

$$\bar{\sigma}_{ij} = \int_S \sigma_{ij}\, dS = \sum_{m=1}^{N_{tir}} \bar{\sigma}_{ij}^{tri} \frac{S_m^{tri}}{S_{RVE}} + \sum_{n=1}^{N_{quad}} \bar{\sigma}_{ij}^{quad} \frac{S_n^{quad}}{S_{RVE}} \tag{2}$$

$$\bar{\varepsilon}_{ij} = \int_S \varepsilon_{ij}\, dS = \sum_{m=1}^{N_{tir}} \bar{\varepsilon}_{ij}^{tri} \frac{S_m^{tri}}{S_{RVE}} + \sum_{n=1}^{N_{quad}} \bar{\varepsilon}_{ij}^{quad} \frac{S_n^{quad}}{S_{RVE}} \tag{3}$$

Where N_{tir} （N_{quad}）is the number of triangular(quadrangular)element, $\bar{\sigma}_{ij}^{tri}$ （$\bar{\sigma}_{ij}^{quad}$）or $\bar{\varepsilon}_{ij}^{tri}$ （$\bar{\varepsilon}_{ij}^{quad}$）is the mean stress or strain in a triangular(quadrangular)

element , $S_m^{tri}(S_n^{quad})$is the area of triangular(quadrangular) element and S_{RVE} is the total area of RVE.

The mean stress and strain of one element are related to the values at every Gaussian integral point in the element. In a triangular element, there is only one Gaussian integral point, and no coordinate transformation, and therefore

$$\bar{\sigma}_m^{tri} = \sigma_{\mathrm{ij}}^I \tag{4}$$

$$\bar{\varepsilon}_m^{tri} = \varepsilon_{\mathrm{ij}}^I \tag{5}$$

where $\sigma_{\mathrm{ij}}^I(\varepsilon_{\mathrm{ij}}^I)$ is the corresponding value of the Gaussian integral point.

In a quadrangular element, $\bar{\sigma}_{ij}^{quad}$和$\bar{\varepsilon}_{ij}^{quad}$ can be solved by

$$\bar{\sigma}_{ij}^{quad} = \int_S \sigma_{ij}\, dS = \sum_I \sigma_{\mathrm{ij}}^I\, |\mathcal{J}(\mathrm{I})| \mathrm{W}（\mathrm{I}） \tag{6}$$

$$\bar{\varepsilon}_{ij}^{quad} = \int_S \varepsilon_{ij}\, dS = \sum_I \varepsilon_{\mathrm{ij}}^I\, |\mathcal{J}(\mathrm{I})| \mathrm{W}（\mathrm{I}） \tag{7}$$

where W（I）=1 and $\mathcal{J}(\mathrm{I})$ is the Jacobian matrix which is

$$\mathcal{J} = \begin{bmatrix} \frac{\partial \chi}{\partial \xi} & \frac{\partial y}{\partial \xi} & \frac{\partial z}{\partial \xi} \\ \frac{\partial \chi}{\partial \eta} & \frac{\partial y}{\partial \eta} & \frac{\partial z}{\partial \eta} \\ \frac{\partial \chi}{\partial \zeta} & \frac{\partial y}{\partial \zeta} & \frac{\partial z}{\partial \zeta} \end{bmatrix} = \begin{bmatrix} \sum \frac{\partial N_i}{\partial \xi} x_i & \sum \frac{\partial N_i}{\partial \xi} y_i & \sum \frac{\partial N_i}{\partial \xi} z_i \\ \sum \frac{\partial N_i}{\partial \eta} x_i & \sum \frac{\partial N_i}{\partial \eta} y_i & \sum \frac{\partial N_i}{\partial \eta} z_i \\ \sum \frac{\partial N_i}{\partial \zeta} x_i & \sum \frac{\partial N_i}{\partial \zeta} y_i & \sum \frac{\partial N_i}{\partial \zeta} z_i \end{bmatrix}$$

$$= \begin{bmatrix} \frac{\partial N_1}{\partial \xi} & \frac{\partial N_2}{\partial \xi} \cdots & \frac{\partial N_m}{\partial \xi} \\ \frac{\partial N_1}{\partial \eta} & \frac{\partial N_2}{\partial \eta} \cdots & \frac{\partial N_m}{\partial \eta} \\ \frac{\partial N_1}{\partial \zeta} & \frac{\partial N_2}{\partial \zeta} \cdots & \frac{\partial N_m}{\partial \zeta} \end{bmatrix} \begin{bmatrix} x_1 & y_1 & z_1 \\ x_2 & y_2 & z_2 \\ \vdots & \vdots & \vdots \\ x_m & y_m & z_m \end{bmatrix} \tag{8}$$

where

$$N_1 = \frac{1}{4}(1+\xi)(1+\eta),$$

$$N_2 = \frac{1}{4}(1-\xi)(1+\eta),$$

$$N_3 = \frac{1}{4}(1-\xi)(1-\eta),$$

$$N_4 = \frac{1}{4}(1+\xi)(1-\eta),\ \ \mathrm{i} = 1,2,3,4.$$

In this way, the mean stress and strain of a whole RVE can be calculated by Eqs. (2)and (3)。

2.2 Surface-based cohesive method

Cohesive technology is widely used in simulation the damage between filler particles and matrix [19]. In this paper, a similar method named surface-based cohesive behavior is introduced to simulate the particles. To simulate the degradation and eventual failure of the bond between two surfaces, a damage model that consists of two ingredients a damage initiation criterion and a damage evolution law is established. In this paper , a typical traction-separation response which is used to simulate the damage between the nano-SiO_2 particles and matrix, which is shown in Fig.1.The available traction-separation model assumes linear elastic behavior followed by the initiation and evolution of damage. The elastic behavior is written in terms of an elastic constitutive matrix which relates the normal and shear stresses to the normal and shear separations across the interface. The elastic behavior can be written as

$$\mathrm{t} = \begin{pmatrix} t_n \\ t_s \end{pmatrix} = \begin{pmatrix} K_n & K_t \\ K_\mathrm{t} & K_s \end{pmatrix} \begin{pmatrix} \delta_n \\ \delta_s \end{pmatrix} \tag{9}$$

where t consists of two components $t_n$and t_s, which represent the normal and the shear traction, respectively. The corresponding separations and denoted byδ_n and δ_s. Matrix K is a constant before damage initiates and it will decrease according to the damage evolution law when damage initiates.

The maximum stress criterion is used as the damage initiation criterion in this paper. It is assumed that damage initiates when the maximum contact stress is equal to the maximum stress. This criterion can be written as

$$MAX\left\{\frac{\langle t_n\rangle}{t_n^{max}},\frac{\langle t_s\rangle}{t_s^{max}}\right\}=1 \tag{10}$$

where $t_n^{max}$and t_s^{max} are the peak values of the contact stress,respectively. The symbol⟨ ⟩is the Macaulay bracket。

When the interface displacement reaches δ_n^{max}, the bond between two surfaces softens through damage evolution. The contact stress components are affected by the damage according to

$$t_n'=\begin{cases}(1-D)t_n & t_n\geq 0\\ t_n & t_n<0\end{cases} \tag{11}$$

$$t_s'=(1-D)t_s \tag{12}$$

where D is a scalar damage variable representing the overall damage at the contact point. For linear softening , $D\ is$ reduced to the following expression

$$D=\frac{\delta_n^f\ (\delta-\delta_n^{max})}{\delta(\delta_n^f-\delta_n^{max})} \tag{13}$$

where the subscript "n" represents the normal or the shear direction andδ_n^{max} refers to the maximum value of the effective separation attained in the loading history.

3.Matericals and experimental procedure

3.1 Matericals

The ABS (757K) and PMMA (CM-211) resins were obtained from Zhenjiang Chimei Chemical Co., Ltd. and Taiwan Chimei Chemical Co., Ltd., respectively. The anano-SiO_2 (VK-SP15C) was purchased from Hangzhou Wanjing New Material. The mean diameters of the nano-SiO_2 particles were approximately 15 nm. Stearic acid and silane coupling agent were provided by Jinan Xingfeilong Chemical Reagent Factory.

3.2 Preparation of blends

All of the materials were dried at 80 °C for 12 h in an air-circulating oven prior to use. ABS/PMMA/nano-SiO_2 was prepared by using a two-screw extruder (L/D ratio of the screw: 40; diameter: 21.7 mm; SJSL-20, China) at 200 °C–225 °C from the hopper to the die. Then, the pellets were dried again in an air-circulating oven at 80 °C for 12 h. The standard testing specimens were processed in a 68-ton injection molding machine (XL680, China). The injection temperature was set at 225 °C–215 °C from the hopper to the nozzle, and the holding pressure was 50 MPa. The mass ratio of ABS to PMMA was fixed at 80/20, and the content of nano-SiO_2 is 2wt%.

3.3 Characterization

The tensile properties were conducted on a CMT 5305 electrical testing machine at room temperature. The crosshead speed was maintained at 4 mm/min.

Scanning Electron Microscope (SEM). The SEM samples for the morphology and fracture mechanism analyses were directly collected from the broken pieces after the mechanical tests. The fracture surface was coated with a thin layer of gold before being observed under a FEI-NOVA NANOSEM 450 SEM.

Transmission Electron Microscope (TEM). The morphological structure was examined by using a TEM (JEM-2100) at an accelerating voltage of 200 KV. The specimens were dyed with a mixture of sulfur, zinc stearate, and promoter (content ratio: 90/5/5) in an oven at 120 °C for 24 h. Then, 100 nm thick samples were prepared through ultra-cryomicrotomy at −100 °C by using a Leica UCT microtome.

4 Finite element model

A representative volume element was used to represent the selected composite microstructure in this paper. The morphology of ABS/PMMA and ABS/PMMA/nano-SiO_2 blends was shown in Fig.2, which was clearly observed using TEM. The rubber particle morphologies are regular and have circle shapes, however, the particle morphologies of nano-SiO_2 are irregular because of aggregation.

The structure modeling of ABS/PMMA/nano-SiO_2 composite was created based on this information. The determination of the minimum accurate RVE size is an extremely laborious work so we just verify that the RVE size used in this paper is reasonable.The size of RVE model was $1\text{mm} \times 1.2\text{mm}$, and the average size of the ruber particles is 0.2mm. The size and shape of nano-SiO_2 were simplified because of its aggregation. The RVE model of ABS/PMMA/nano-SiO_2 was shown in Fig.3. Note that the model generated here is a special one, in which no particles cross the surface. This is the limitation for surface-based cohesive element in Abaqus to simulate the ABS/PMMA/nano-SiO_2 composite. In terms of the finite element discretization, the general linear solid element C3D8R in Abaqus was used to mesh the matrix and the nano-SiO_2 particles. The surface-based cohesive element was adopted to account for the interface behavior between matrix and particles .The meshing of representative volume unit was shown in Fig. 4.

The parameters of Cohesive behavior and Damage should be selected before using Surface-based Cohesive to define the boundary condition. In this paper, the above

parameters were given based on the relevant literatures [20-23],because it is difficult to define the parameters through our experience. They were listed in table1. Meanwhile，we only considered the elastic stage of nano-SiO_2 because of its high yield strength and elastic modulus relative to the PMMA and ABS. PMMA and ABS are input corresponding elastic-plastic properties respectively.

5 Numerical results and discussion

A visible stress and strain evolution, as well as the crack generation and propagation inside the composite during tensile loading we shown in Fig.5 and Fig.6, respectively. Analyzing the numerical model, one could find that the first fracture behavior happened between nano-SiO_2 particles and matrix when ε was 0.05, and the damage area was becoming larger with increasing the value of ε.

In this simulation, We can identify that the initial stage of high stress area occurs at the interface between nano-SiO_2 particles and matrix. During the composite deformation, as shown in Fig.5, the aggregation nano-SiO_2 particles act as stress concentration points. When ε was 0.075，the high stress area occurred in the equator of rubber particles . One can see that the high stress area of rubber particles is gradually expanding from the rubber equator to the poles, with the increase of extension area, rubber particles caused further interface debonding behavior between the matrix.

Fig.6 presented the different stages of the equivalent plastic strain with increasing the load. The plastic deformation zone was started from the interface between the nano-SiO_2 particles and matrix. The deformation area attracted to each other and had mutual connection under the influence of adjacent nano-SiO_2 aggregations.It was obvious shown that the connection road was along 45 ° direction.

One can find that the aggregation of nano-SiO_2 and weak interface bonding with matrix promote easier interface debonding, which decreases the stiffness and strength of ABS/PMMA/nano-SiO_2 composite. The SEM micrograph in Fig.7 shows the morphology of an actual fracture section , the fracture direction is about 45°，which is consistent with the direction observed in the numerical model.

6 conclusions

A microstructure-based finite element model was developed to predict the deformation and fracture behavior of ABS/PMMA/nano-SiO_2 composites. The validity of the modeling results were justified by the agreement of the fracture surface morphology with those predicted by the simulation. A visible process of elasto-plastic deformation along with crack generation and propagation was described, which is helpful for the study of deformation and fracture mechanisms in ABS/PMMA/nano-SiO_2 composites. Some salient conclusions from our work are summarized as follows:(1) tensile fracture in the ABS/PMMA/nano-SiO_2 blends is initiated by nano-SiO_2 particles which is debonding from matrix as a result of stress concentration.(2) Weaker interfaces promote easier interface debonding, decrease the composite's stiffness and strength.(3) nano-SiO_2 particles lead to fracture along 45° direction, the simulation result is consistent with the experimental result.

Acknowledgments

The authors sincerely acknowledge the financial supports by Natural Science Foundation of Shandong Province (grant no.ZR2020KF024.), the university Research

Project of Shandong Province (grant no.J17KB007), and Natural Science Foundation of Shandong Jiaotong University (grant no.Z201937).

Declarations

Conflict of interest the authors state that there are no conflicts of interest.

References

1. A.M.Zhang, G.Q.Zhao, Y.J.Guan, Mechanical and Thermal Properties of ABS / PMMA /Potassium Titanate Whisker Composites.Polym.Plast. Techno l. Eng .56, 382-390(2016)

2. B.K.KIM, X.M.Xie, L.K.YOON, Effects of Annealing in ABS Ternary Blends. J.Appl. Polym. Sci.66,1531-1542(1997)

3. E.Correa Gómez, G.M.Domínguez Almaraz, J.C.Verduzco Juárez ,Crack initiation and propagation on CT specimens of two polymers (ABS and PMMA), under cyclic constant displacement loading. Theor. Appl.Fract.Mec. 100,55-64(2019)

4. S.A.Shishavan, T.Hasanzadeh, R.M.Moradian, Comprehensive Investigation of Morphological Properties of ABS/Nanoclay/PMMA Polymeric Nanocomposite Foam. Polym.Sci. Ser. A. 61, 334-344(2019)

5. G.C.Maries, D.Bungau, C.Costea, T.Moldovan, Determining the Influence of the Processing Temperature by Injection and of the Subsequent Pressure on the Surface's Hardness and Indentation Modulus of the Products Made of HDPE, PMMA, PC plus ABS through Nanoindentation - G-Series Basic Hardness Modulus at a Depth Method. Mater.Plastic. 54,214-220(2017)

6. W.Y.Dong, F.L.Ren, M.F.Zhang, J.Q.Wang, Y.J.Li, Phenomenon of LCST-type phase

behavior in SAN/PMMA systems and its effect on the PLLA/ABS blend compatibilized by PMMA-type polymers: Interface stabilization or micelle formation.Polym. 163,36-47(2019)

7. W.Zhang, X.Xu, H.Wang, F.Wei, Y.Zhang, Experimental and numerical analysis of interfacial bonding strength of polyoxymethylene reinforced cement composites. Constr. Build. Mater. 207,1-9(2019)

8. A.M.Zhang, G.Q.Zhao, Y.J.Guan, Effect of Surface Modifiers and Surface Modification Methods onProperties of Acrylonitrile–Butadiene–Styrene/Poly (methylmethacrylate) /Nano-Calcium Carbonate Composites .J.Polym.Compos. 80,2523-2532(2013)

9. J.Zhao, H.Li, G.Cheng, Y.Cai, On predicting the effective elastic properties of polymer nanocomposites by novel numerical implementation of asymptotic homogenization method.Compos.Struct. 135,297-305(2016)

10. J.Zhang, Q. Ouyang, Q.Guo, Z.Li, G.Fan, Y.Su, L.Jiang, E.J.Lavernia, J.M.Schoenung, D.Zhang, 3D Microstructure-based finite element modeling of deformation and fracture of SiCp/Al composites.Compos. Sci .Techol. 123,1-9(2016)

11. P.Sheng, J.Zhang, Z.Ji, An advanced 3D modeling method for concrete-like particle-reinforced composites with high volume fraction of randomly distributed particles.Compos. Sci. Techol. 134,26-35(2016)

12. A.Pontefisso, M.Zappalorto, M.Quaresimin, An efficient RVE formulation for the analysis of the elastic properties of spherical nanoparticle reinforced polymers. Comput.Mater. Sci. 96,319-326(2015)

13. Z.Yuan, F.Li, F.Xue, M.He, M.Z.Hussain, Analysis of the stress states and interface damage in a particle reinforced composite based on a micromodel using cohesive elements.Mater.Sci. Eng. A. 589,288-302(2014)

14. H.Xiu, Selective localization of titanium dioxide nanoparticles at the interface and its effect on the impact toughness of poly(L-lactide)/poly(ether)urethane blends . Exp.Polym.Lett. 7,261-271(2013)

15. J.Mu, Y.Zhou, X.Bu, T.Zhang, Preparation and Characterization of Micron-Sized PMMA/SiO_2Composite Microspheres.J.Inorg.Organomet. 24,776-779(2014)

16. A.Haghtalab, S.Rahimi, Study of viscoelastic properties of nanocomposites of SiO2–acrylonitrile–butadiene–styrene.J. Appl.Polym.Sci. 127,4318-4327(2013)

17. J.Ding, Z.M.Yue, J.Sun, J Gao. Effects of nano-silicon dioxide surface modification on the morphology and mechanical properties of ABS/PMMA blends. J. Polym.Eng. 38,617-623(2018)

18. N.VuBac, T.Lahmer, H.Keitel, J.Zhao, X.Zhuang, T.Rabczuk, A unified framework for stochastic predictions of mechanical properties of polymeric nanocomposites. Mech. Mate. 68,70–84(2014)

19. S.T.Liu, G.D.Cheng, Homogenization method of stress analysis of composites strurcture.*China*.J.Theor. Appl.Mech. 29,306-313(1997)

20. M.Tijssens, E.van der Giessen, L.J.Sluys, Modeling of crazing using a cohesive surface methodology. Mech.Mater. 32,19-35(2000)

21. G.A.Maltin, B. L.Sluys, E.Giessen, Numerical simulation of quasi-brittle fracture using damaging cohesive surfaces. Euro.J. Mech. A. 19,761-779(2000)

22. J.K.Zhang, X.Zhang, Simulating low-velocity impact induced delamination in composites by a quasi-static load model with surface-based cohesive contact. Compos.Struct. 125,51-57(2015)

23. M.Sagaei, M.Baniassadi, S.Ahzi, M.MOsavi, F.Pourboghrat, An interfacial debonding-induced damage model for graphite nanoplatelet polymer composites. Comput.Mater.Sci. 96,191-199(2015)

Figures

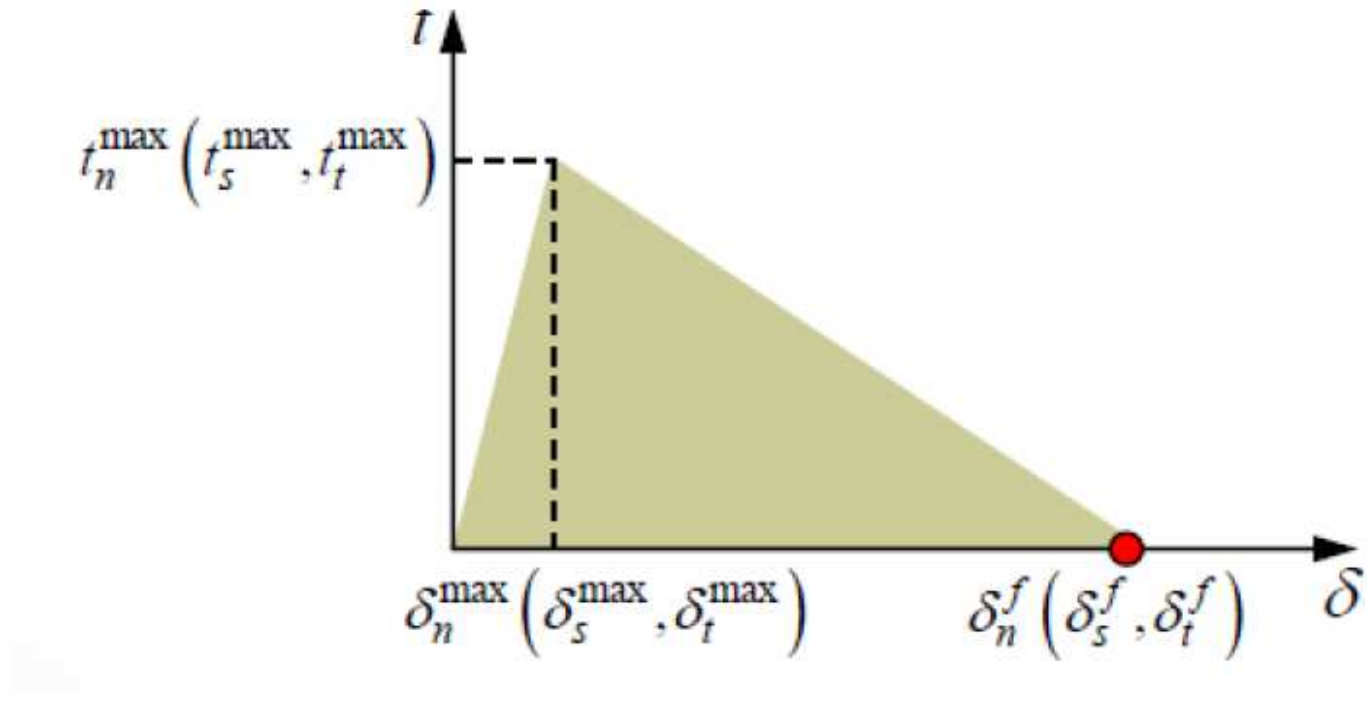

Figure 1

Damage modeling for cohesive surface

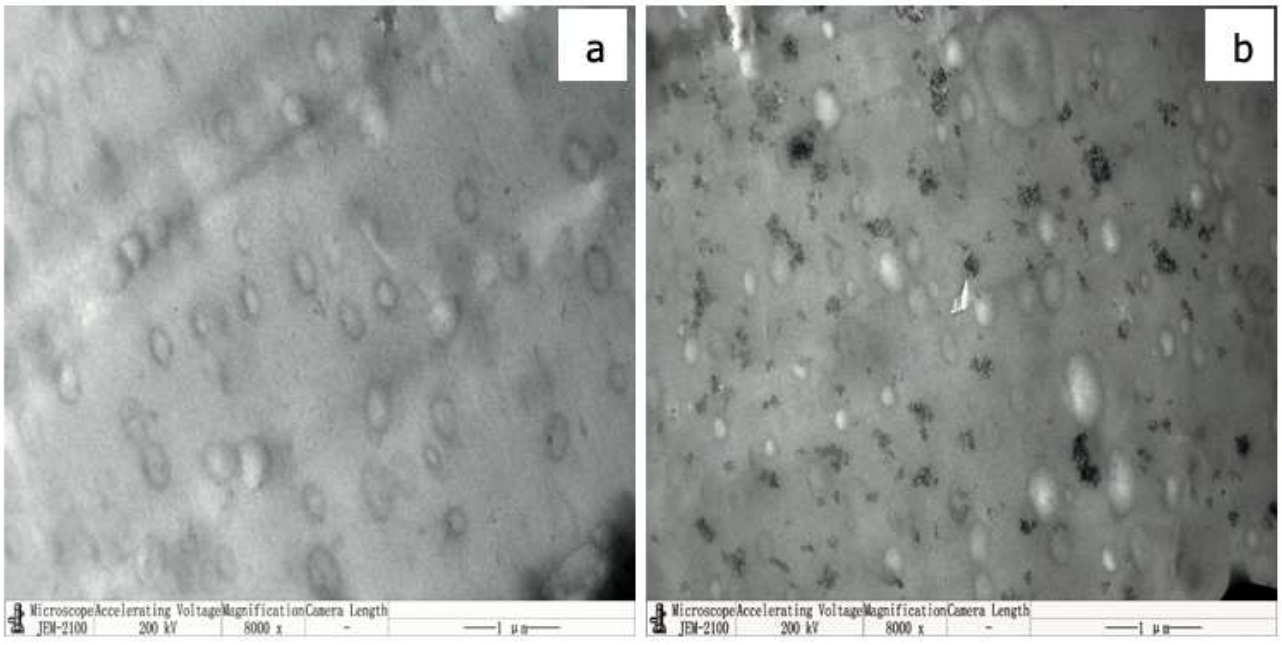

Figure 2

Morphology of ABS/PMMA and ABS/PMMA/nano-SiO2 (a) ABS/PMMA,(b) ABS/PMMA/nano-SiO2

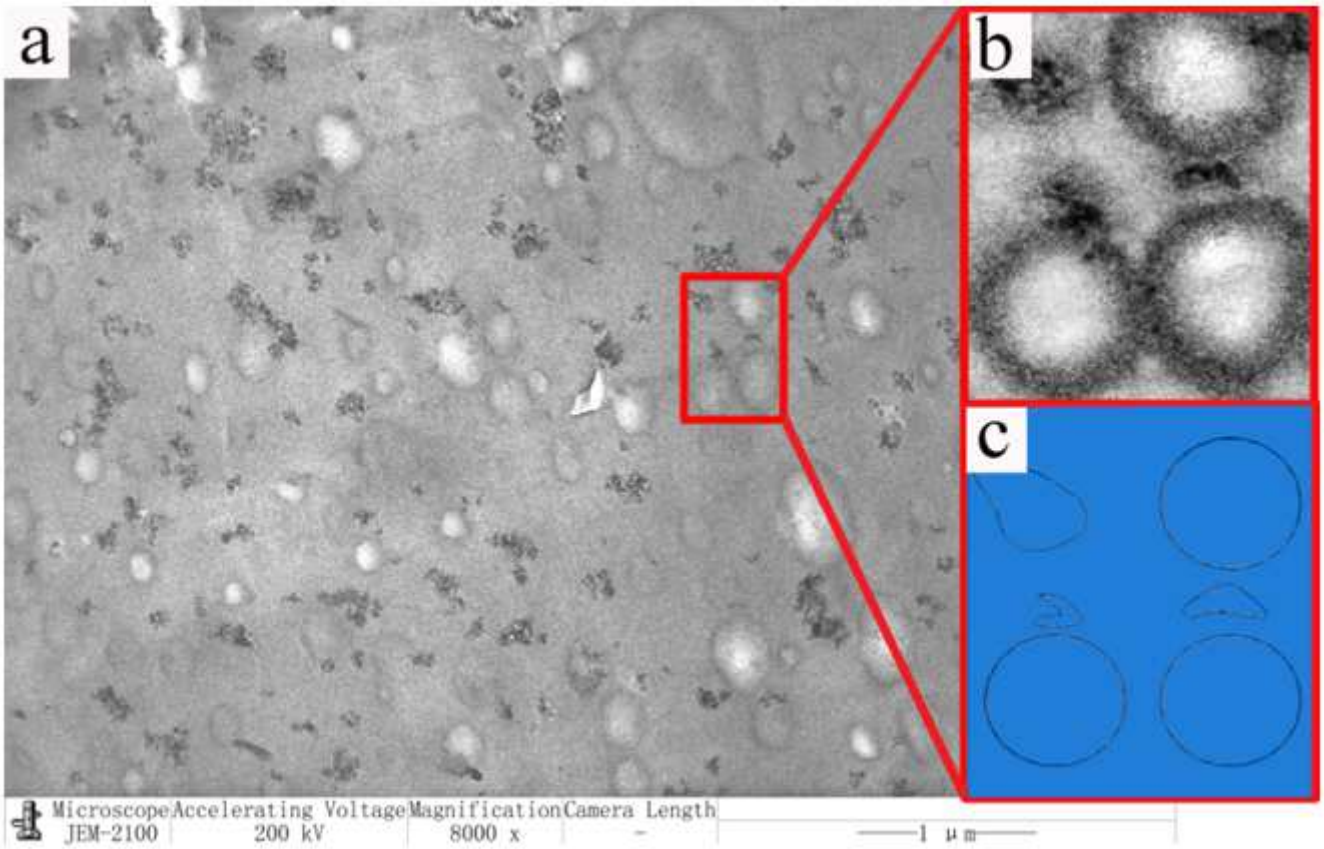

Figure 3

The RVE model of ABS/PMMA/nano-SiO2

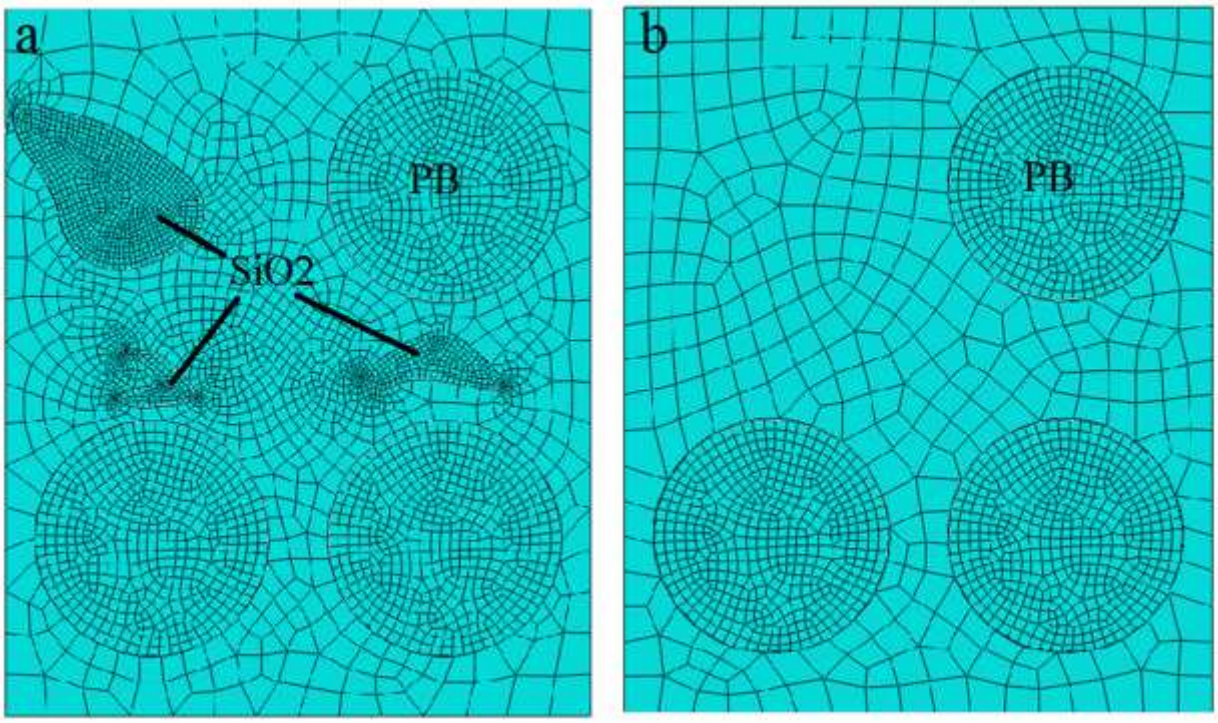

Figure 4

The meshing of representative volume unit.(a) ABS/PMMA (b) ABS/PMMA/ nano-SiO2

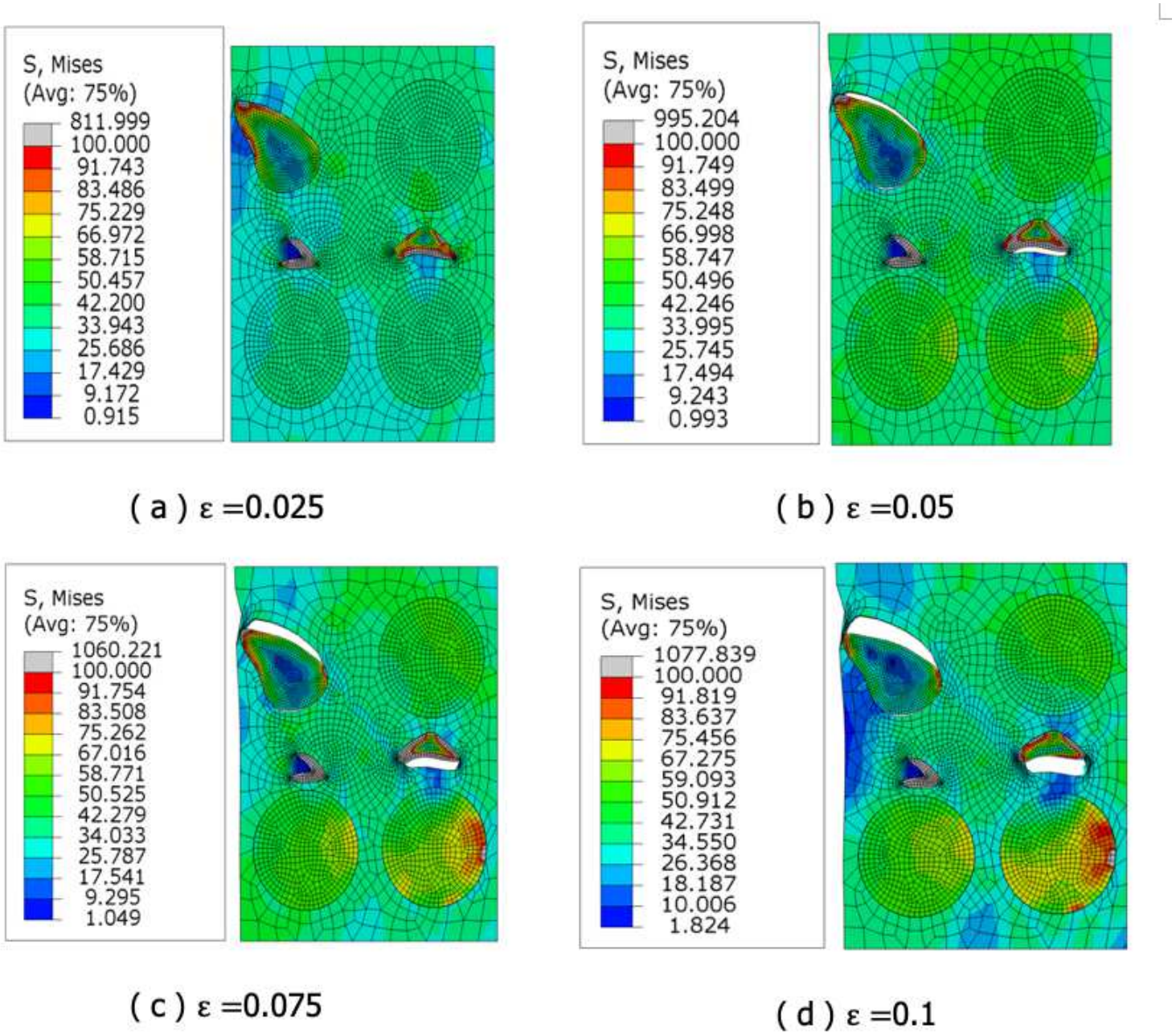

Figure 5

Stress evolution and damage process inside the ABS/PMMA/nano-SiO2 blend during tensile deformation

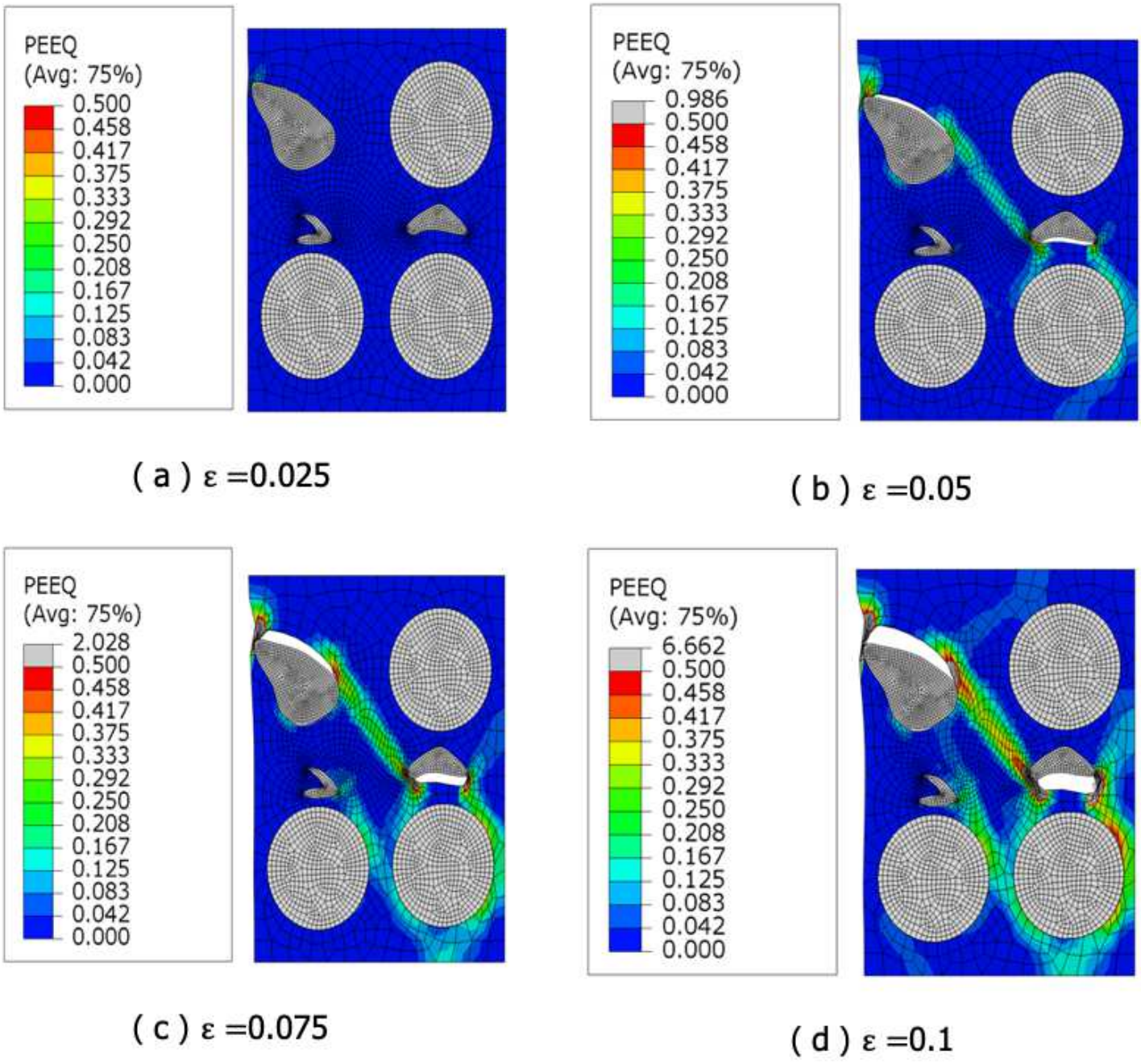

Figure 6

Stress evolution and damage process inside the ABS/PMMA/nano-SiO2 blend during tensile deformation

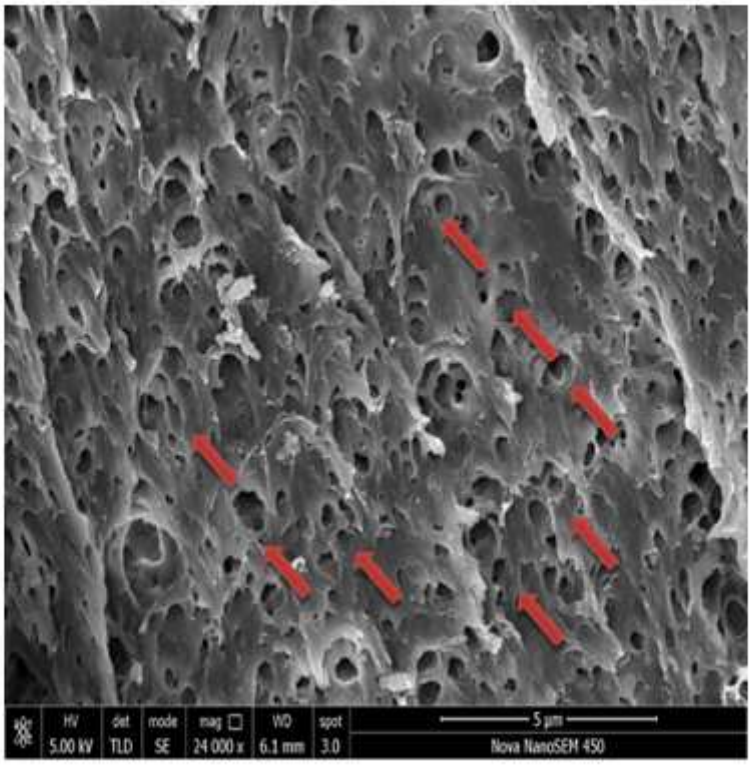

Figure 7

SEM micrograph of tensile fracture surface ABS/PMMA/nano-SiO2

Supplementary Files

This is a list of supplementary files associated with this preprint. Click to download.

- table.docx